Article citation info:
Szpica D, Gęca MS, Hunicz J, Jakubowski M, Krzemiński A. Mieczkowski G. Cycle-by-cycle performance evaluation of a diesel engine fueled with a mixture of hydrotreated vegetable oil mixed with waste plastic pyrolysis oils. Combustion Engines. 2025;202(3):109-117. https://doi.org/10.19206/CE-207383

Dariusz SZPICA
Michał S. GĘCA
Jacek HUNICZ
Mirosław JAKUBOWSKI
Artur KRZEMIŃSKI
Grzegorz MIECZKOWSKI

Combustion Engines
Polish Scientific Society of Combustion Engines

Cycle-by-cycle performance evaluation of a diesel engine fueled with a mixture of hydrotreated vegetable oil mixed with waste plastic pyrolysis oils

ARTICLE INFO

Received: 28 April 2025
Revised: 14 June 2025
Accepted: 20 June 2025
Available online: 7 July 2025

Changing regulations on emissions from propulsion sources used in transportation and closed-loop resource management are intensifying the search for substitute fuels, especially for compression-ignition engines. In the study, three fuels were tested for comparison: conventional diesel fuel (DF), hydrotreated vegetable oil (HVO), and a mixture of HVO with waste pyrolytic oils from polypropylene (PPO) and polypropylene (PSO) in 60/20/20 weight ratios (HVO + WPPO). Tests were conducted on a specialized platform with an AVL 5402 engine, analyzing their combustion and operating stability under two different load and speed conditions. The results showed that HVO and the HVO + WPPO mixture exhibit similar or even better combustion performance compared to DF. Some differences were found in cylinder pressure traces, indicated mean effective pressure and heat release. Statistical analyses, including ANOVA and Levene's tests, confirmed significant differences between the fuels, indicating the potential of the HVO + WPPO mixture as an environmentally friendly alternative. The determined coefficients of variation allowed an assessment of the stability of engine operation. In conclusion, the research suggests that both HVO and its mixture with PPO and PSO can be effective and environmentally friendly solutions for diesel engines, with the possibility of wide application in the future.

Key words: *alternative fuel supply, hydrotreated vegetable oil, waste plastic pyrolytic oils, combustion, research*

1. Introduction

A very popular source of propulsion for motor vehicles and work machinery is the compression-ignition engine because of its relatively high efficiency, reliability, low fuel consumption, and ease of adaptation [10, 16, 29, 30]. However, the disadvantage of this type of propulsion is the emission of pollutants, including CO, NO_x, and PM. In addition, fossil fuels account for 85% of CO_2 emissions and 64% of total greenhouse gas emissions [5, 25]. Therefore, internal combustion engines are subject to increasingly stringent rules and regulations regarding the emission of toxic compounds from exhaust [11, 15].

One method for reducing toxic compounds and CO_2 emissions is to develop alternative waste-derived fuels. This group of fuels includes HVO and TPO, which are combinations of aromatic and aliphatic compounds, and plastic fuels (PPO and PSO) obtained by pyrolysis [4, 13, 14].

HVO can be produced from waste biomass, such as animal fats and vegetable oils. This fuel did not contain sulfur or aromatic hydrocarbons. HVO, compared to conventional diesel, has a higher cetane number and lower viscosity and density compared to conventional diesel. The high cetane number of hydrogenated vegetable oils accelerates the onset of combustion, particularly at low and medium loads [17]. The use of HVO to power a compression-ignition engine results in a 40% reduction in NO_x and PM emissions compared with diesel [12, 18].

To date, engine tests have been conducted on HVO alone and diesel mixtures with 30% and 7% v/v HVO [26]. Engine tests on mixtures of diesel, HVO, rapeseed methyl ether, and n-octanol isomers have also been conducted [20].

The authors of [21] showed a reduction in CO emissions by more than 50% when feeding the engine during the cold start phase with a mixture of DF and HVO (30%). No significant differences were observed in NO_x emissions compared to DF, whereas PM was reduced by 5.2–11.8%, depending on the test conditions.

Fuel obtained from waste plastic oil can be used in a compression-ignition engines at a higher compression ratio than that obtained from DF without any modifications to the power unit [1].

The results of ongoing research indicate that the use of fuels with the addition of plastic waste oil in a compression-ignition engine decreases the thermal efficiency by more than 2% compared with pure DF [7].

In [3], the authors demonstrated a positive or neutral effect of HVO on most of the measured emission components and engine operating parameters. Decreases of several tens of percent were observed in CO, THC, PM, and smoke emissions. NO_x and CO_2 emissions decreased, and the power output increased by a few percent.

In the case of using plastic pyrolytic oil (PPO), the results obtained by researchers are divergent, particularly in the context of NO_x emissions, with some studies reporting a reduction of more than 63%, whereas others reported an increase of more than 44% compared to running on pure DF [8].

Studies on mixtures of PPO with DF at concentrations of 10, 20% and 30% PPO showed that at 20%, the engine achieved a slightly higher thermal efficiency than that of pure DF [6]. It was further shown that NO_x and HC emissions were lower at low loads and increased with increasing load compared with DF.

Researchers [24] used a mixture of PPO and DF in proportions up to 50% PPO and showed that a higher concentration of PPO in the mixture increased the engine thermal efficiency and reduced the specific fuel consumption.

In the literature, one can find a PPO designation associated with pyrolytic oil extracted from plastic or made from polypropylene. The above data related to PPO oil refers to the first meaning. With regard to pyrolytic oil extracted from polypropylene, the authors of [22] showed that the addition of 20% PPO in a mixture with DF had no significant effect on HC and CO emissions, whereas the admixture of PSO increased them.

TPO can be used in fuel compression ignition engines as a mixture with diesel fuel (from 10% to 90%) without changing the engine design.

Combustion stability is crucial to overall engine performance because a mixture of fuels with different autoignition properties can increase the variability of the combustion cycle [23]. The available literature lacks studies on the combustion stability of HVO mixtures containing PPO and PSO. The research gap has directed efforts to develop an alternative fuel that is a mixture of these fuels. This type of activity is contained within a closed loop of raw materials. An important feature of the developed mixture is the similarity of its ignition and combustion characteristics to those of DF. The scientific contribution of such an activity is the evaluation of the preservation of the stability of the engine operation fueled by the developed mixture, which guarantees the functional continuity of the propulsion source.

2. Materials and methods

2.1. Tested fuels

In this study, three diesel fuels were tested.

- conventional diesel fuel (DF)
- hydrotreated vegetable oil (HVO)
- a mixture containing 60 wt% HVO, 20 wt% PPO and 20 wt% PSO (HVO + WPPO).

Table 1. Basic technical parameters of the tested fuels

Property	Unit	Diesel	HVO	PPO	PSO
Density at 15°C	kg/m^3	828	778	761	937
Kinematic viscosity (40°C)	mm^2/s	2.94	2.86	1.77	1.70
Lower heating value	MJ/kg	43.6	44	42.4	41
Flash point	°C	66	68	29	< 19
Cetane number	–	55	90	28	≈0
Composition by mass:					
Carbon	%	86.7	84.5	87.8	91
Hydrogen	%	13.1	15.2	12.2	8.2
Oxygen	%	0.05	–	–	–
Aromatic	%	17	< 1	–	98
FAME	%	6.3	–	–	1
Sulfur	ppm	5.2	–	56	3

The DF used as the base fuel was an EN 590-compliant conventional fuel from the ORLEN distribution network. HVO was a fuel derived from the hydrotreatment of vegetable oil and was distributed by NESTE. PPO was derived from the pyrolysis of polypropylene, whereas PSO was derived from the pyrolysis of polystyrene. The HVO + WPPO mixture was developed to achieve a similar ignition delay, volatility, and viscosity to DF. All component fuels were subjected to detailed physicochemical analyses to aid in mixture formation (Table 1).

2.2. Test equipment

Experiments were conducted using a single-cylinder AVL 5402 research engine. The primary operating parameters are listed in Table 2. A schematic of the test bench, detailing the air and fuel flow paths, is shown in Fig. 1.

Table 2. Research engine specifications

Parameter	Value/specification
Engine model	AVL 5402
Operating cycle	single-cylinder, four-stroke
Cylinder bore	85 mm
Piston stroke	90 mm
Connecting rod length	138 mm
Total displacement	510.5 cm^3
Compression ratio	17:1
Number of valves	4
Swirl number	1.7
Fuel delivery method	direct injection
Injection system	Bosch CP4.1, common rail
Injector type	electromagnetic, 8-hole, 0.12 mm orifice, 151 deg spray angle
Max. injection pressure	180 MPa
Natural gas supply	M+W D-6300 mass flow controller
Boost system	Eaton M45, electrically powered
EGR configuration	high-pressure loop, with cooling
ECU and control system	Bosch ETK7 with AVL-RPEMS
Intake valve opens at	712 CAD
Intake valve closes at	226 CAD
Exhaust valve opens at	488 CAD
Exhaust valve closes at	18 CAD
Max. IMEP	2.4 MPa

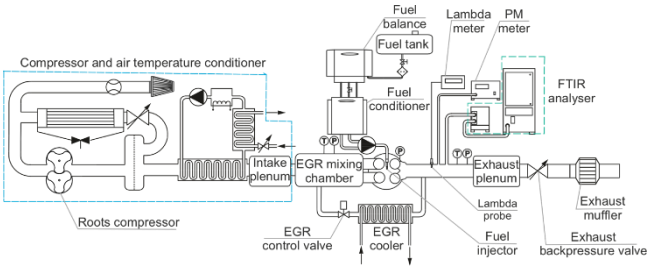

Fig. 1. Diagram of the engine air and fuel paths

The engine incorporated a four-valve cylinder head and a toroidal combustion chamber formed within the piston. The fuel was delivered using a Bosch CP 4.1 high-pressure pump to an eight-hole solenoid injector with a spray angle of 151 deg. The injection process was managed using ETAS INCA software and an open Bosch electronic control unit (ECU).

The fuel temperature and flow were regulated using an AVL 753C temperature controller and an AVL 733S dynamic flow meter. The boost pressure was generated using an Eaton M45 Roots-type supercharger powered by an 11 kW electric motor. The compressed intake air was thermally stabilized using a system of heat exchangers and a mixing valve.

An exhaust backpressure valve was used to emulate the effect of a turbocharger, facilitating high-pressure exhaust gas recirculation (EGR) and preventing the scavenging of natural gas during valve overlap.

The coolant and engine oil temperatures were maintained with ±0.5°C accuracy using a dedicated thermal management system. The air-fuel ratio was measured using a Bosch LSU 4.2 lambda sensor and an ETAS LA4 lambda meter with pressure compensation.

Combustion diagnostics relied on in-cylinder pressure data obtained from an AVL GU22C piezoelectric pressure sensor, synchronized with an optical encoder providing 0.1 CAD resolution.

Exhaust gas analysis of both the regulated and unregulated compounds was performed using an AVL FTIR spectrometer. The size distribution of particulate matter was measured using a TSI EEPS 3090 spectrometer operating on the principle of electrical mobility, covering the (5.6…560) nm range across 32 size bins. The key parameters of the measurement system are presented in Table 3.

Table 3. Engine test bench measurement equipment and accuracy

Parameter measured	Device	Meas. range	Accuracy
In-cylinder pressure	AVL GU22C	0…25 MPa	±0.25…1.0%
Liquid fuel consumpt.	AVL 733S	0…1.25 kg/h	±0.12%
Gaseous fuel flow	M+W D-6300	0…120 NL/min	±2%
Lambda (AFR)	Bosch LSU 4.2/ETAS LA4	0.7…2.8	±1.5%
Air mass flow rate	E+E EE741	2.6…1000 kg/h	±3%
Pressure (int./exh.)	WIKA A-10	0…4 bar	±0.5%
Temperature	TP-361	–40…400 degC	±0.2%
Exhaust gas temp.	TP-204	0…1200 degC	±0.8%
CO emissions	AVL FTIR	1…10000 ppm	±0.36%
UHC emissions	AVL FTIR	1…1000 ppm	±0.1…0.49%
NOx emissions	AVL FTIR	1…4000 ppm	±0.31%
Particulate matter/ number	TSI EEPS 3090	5.6…560 nm	-

2.2. Research and inference methodology

DF, HVO, and HVO + WPPO tests were conducted on a test platform with an AVL 5402 engine at two World Harmonized Stationary Cycle (WHSC) operating points. Low load and low speed were represented by the 1100/25 point, whereas high speed and high load were represented by the 1800/70 point. The first component of the test point designation was the engine crankshaft speed, while the second was the percentage of maximum load, which in this case was 2.2 MPa (BMEP). In the cases analyzed, the averaged BMEP value was 1100/25 – 0.5 MPa, 1800/70 – 1.4 MPa, respectively. In total, 100 consecutive cycles were performed.

In all tests, the 8-hole injector along the common-rail system was controlled using an open control unit in accordance with the modern EPA Tier IV emission standards.

In the first stage of the analysis, the cylinder pressure traces were recorded as functions of the crankshaft angle (CAD). The pressure changes represent the result of a number of input factors and form the basis for evaluating the self-ignition of fuels, the course of their combustion, and other factors determining the engine's energy, environmental, or economic capabilities.

Furthermore, based on the pressure traces and information on the changes in cylinder geometry, the IMEP (Eq. (1)) was calculated, which is the quotient of the volumetric work of the circuit and displacement volume of the cylinder.

$$\mathrm{IMEP} = \frac{\mathrm{W}}{\mathrm{V_{sc}}} = \frac{1}{\mathrm{V_{sc}}} \int \mathrm{p dV_{sc}} \tag{1}$$

where W is the volume work of the cycle; V_{sc} is the swept volume per cylinder; p is the cylinder pressure.

The data used for the IMEP calculations allowed us to assess the heat release (Eq. (2)).

$$\mathrm{q} = \frac{\kappa}{\kappa-1}\mathrm{pdV} + \frac{\kappa}{\kappa-1}\mathrm{Vdp} \tag{2}$$

where κ is the adiabatic exponent, which is the quotient of the specific heat at constant pressure to the specific heat at constant volume (c_p/c_v) determined by considering the effect of temperature and the chemical composition of the charge in the cylinder.

The stability of the cycle-by-cycle engine operation was evaluated using the coefficient of variation (Eq. (3)) [2, 19, 27].

$$\mathrm{COV} = \left(\frac{\sigma}{\bar{\mathrm{x}}}\right) \times 100\% \tag{3}$$

where σ is the standard deviation; $\bar{x}$ is the mean value of the parameter under study.

The standard deviation was calculated using Eq. (4).

$$\sigma = \sqrt{\frac{1}{\mathrm{N}-1}\sum_{\mathrm{i}=1}^{\mathrm{N}}(\mathrm{x_i} - \bar{\mathrm{x}})^2} \tag{4}$$

The average value of the parameter according to Eq. (5).

$$\bar{\mathrm{x}} = \frac{1}{\mathrm{N}}\sum_{\mathrm{i}=1}^{\mathrm{N}} \mathrm{x_i} \tag{5}$$

where N is the number of points assessed; x_i is the value in each i-point.

The following values were considered for the engine stability analysis:

– maximum pressure in the cylinder – p_{max}
– indicated mean effective pressure – IMEP
– maximum heat exerted in the cylinder – q_{max}.

For each of these parameters, the coefficient of variation was determined from the standard deviation and mean value (Eq. (6)–(8)).

$$\mathrm{COV_{p_{max}}} = \left(\frac{\sigma}{\bar{\mathrm{x}}}\right)_{\mathrm{p_{max}}} \times 100\% \tag{6}$$

$$\mathrm{COV_{IMEP}} = \left(\frac{\sigma}{\bar{\mathrm{x}}}\right)_{\mathrm{IMEP}} \times 100\% \tag{7}$$

$$\mathrm{COV_{q_{max}}} = \left(\frac{\sigma}{\bar{\mathrm{x}}}\right)_{\mathrm{q_{max}}} \times 100\% \tag{8}$$

3. Results and analysis

By compiling the sample pressure traces at the first 1100/25 test points (Fig. 2a), the difference in shape between HVO + WPPO relative to DF and HVO was apparent. The reasons for the differences in the pressure traces were correlated with heat evolution (Fig. 2b). It should be noted that the high reactivity of HVO affects the combustion of pilot doses of 1 and 2. The heat evolution process developed 1°CA in advance relative to the DF with a similar gradient. This is different for HVO + WPPO, which lagged by approximately 2°CA behind the DF. The separation of pilot doses was evident in the cases of DF and HVO. A possible reason for this could be that the temperature in the cylinder increased after pilot injection 1, which promoted immediate ignition of the next dose. The burning of pilot fuel 1 increased the temperature and left active radicals,

which caused immediate ignition of the next fuel dose. For the combustion of the main DF and HVO fuel doses, although there is mostly overlap, HVO starts at a lower q value, similar to that of HVO + WPPO. There was a noticeable angular shift in the heat release when the main dose of the HVO + WPPO fuel was burned, as can be seen in the pressure trace (Fig. 2a). The angular shift can affect the IMEP values.

The situation was different at the second 1800/70 test point (Fig. 3a). The exemplary DF pressure trace was below the HVO and HVO + WPPO. The heat development at test point 1800/70 (Fig. 3b) showed a much higher reactivity of HVO, especially at pilot dose 1, where in this particular case it exceeded the value achieved when burning the main dose. Increasing the speed and load of the engine highlighted the separation of pilot doses resulting from the higher brake drag torque, which determines the acceleration of the engine's crank-piston system in addition to the inertia of the mechanical system.

The averaged values from 100 cycles of $\bar{p}_{max}$ (Fig. 4) were 7.848, 7.781 MPa, and 7.556 MPa for DF, HVO, and HVO + WPPO, respectively (Table 4). This represents a 0.85% lower value for HVO and a 3.72% lower value for HVO + WPPO relative to the reference fuel DF. The calculated average values from 100 cycles $\overline{IMEP}$ of (Fig. 4) reached values for DF, of 0.667 MPa, for HVO of 0.659 MPa and for HVO + WPPO of 0.668 MPa, respectively (Table 4). In this case, the percentage difference in HVO relative to the reference DF was 1.26%. HVO+WPPO showed IMPE compliance with DF, with a difference of only 0.07% compared to the disadvantage of DF. The averaged maximum heat discharge $\bar{q}_{max}$ from 100 cycles was 2.05% lower for HVO (56.61 J/deg) and 12.68% lower for HVO + WPPO (50.47 J/deg) relative to DF (57.80 J/deg).

At the second 1800/70 test point, the highest value averaged over 100 cycles of $\bar{p}_{max}$ (Fig. 5) was recorded for HVO + WPPO, it was 12.42 MPa (4.28% higher than the DF reference fuel, 11.906 MPa) (Table 4). HVO showed 12.13 MPa (1.88% higher than that of DF). The 100-cycle averaged value $\overline{IMEP}$ of 1.636 MPa showed HVO + WPPO's advantage over DF (3.28% increase). HVO achieved an IMEP of 1.628 MPa, which was above the 1.584 MPa achieved by DF (2.79% difference). A significant difference from the 1100/25 test point was the change in the main fuel combustion dose. At the 1800/70 point, the highest values averaged over 100 cycles of exerted heat $\bar{q}_{max}$ (Fig. 5) were recorded for HVO (68.20 J/deg, 11.48% increase over DF, 61.18 J/deg). HVO + WPPO also showed an advantage over DF (66.74 J/deg, 9.09% increase) – Table 4.

Table 4. Comparative values of the analyzed parameters at both operating points

Fuel	DF	HVO	HVO + WPPO	DF	HVO	HVO + WPPO
RPM/load	1100/20			1800/70		
$\bar{p}_{max}$, MPa	7.848	7.781	7.556	11.906	12.131	12.416
$\sigma_{p_{max}}$, MPa	0.047	0.045	0.059	0.058	0.136	0.095
$COV_{p_{max}}$, %	0.604	0.573	0.785	0.491	1.122	0.767
$\overline{IMEP}$, MPa	0.667	0.659	0.668	1.584	1.628	1.636
σ_{IMEP}, MPa	0.008	0.007	0.013	0.012	0.033	0.018
COV_{IMEP}, %	1.117	1.101	1.905	0.781	2.006	1.125
$\bar{q}_{max}$, J/deg	57.799	56.612	50.467	61.181	68.203	66.743
$\sigma_{q_{max}}$, J/deg	1.679	1.430	1.520	1.615	2.631	2.076
$COV_{q_{max}}$, %	2.904	2.526	3.011	2.640	3.858	3.110

The highest values of pressure coefficient of variation $COV_{p_{max}}$ at the first test point (1100/25) were recorded for HVO and amounted to 0.573%, which represented a 5.19% increase relative to DF (0.604%) (Table 4). HVO + WPPO showed an increase in the coefficient of variation relative to DF of 29.84% (0.785%). COV_{IMEP} variability differences relative to DF appeared in a similar pattern (1.117%). HVO obtained a value that was 1.48% lower (1.101%), whereas that of HVO + WPPO was 70.49% higher (1.905%). Also, the coefficient of variation $COV_{q_{max}}$ reached the lowest value for HVO (2.526%), 13.00% lower than DF (2.904%). HVO + WPPO had a 3.70% (3.011%) higher rate than that of the DF.

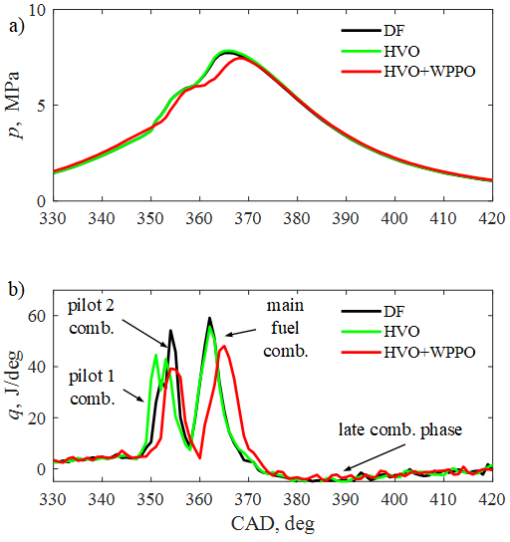

Fig. 2. Examples of in-cylinder pressure traces (a) and heat release (b) at operating point 1100/25

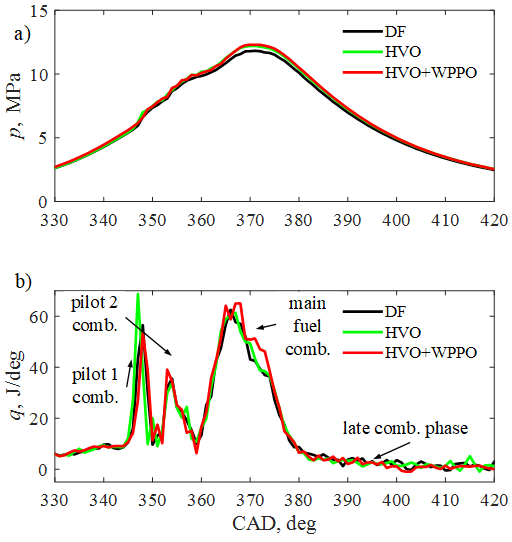

Fig. 3. Examples of in-cylinder pressure traces (a) and heat release (b) at test operating 1800/70

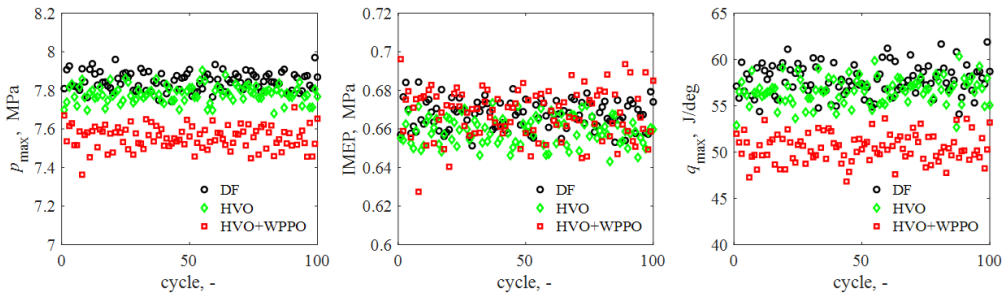

Fig. 4. Comparative values of analyzed parameters at operating point 1100/25

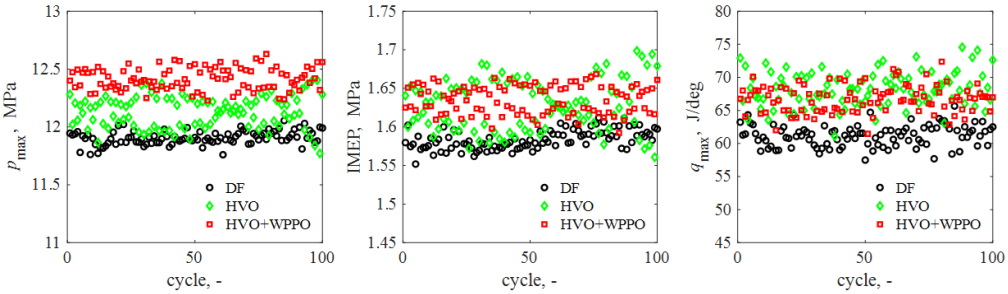

Fig. 5. Comparative values of analyzed parameters at operating point 1800/70

At the second test point (1800/70), where DF achieved lower average values of the compared parameters than the other tested fuels, it also exhibited the smallest variation in these parameters (Table 4). They amounted to $COV_{p_{max}}$ 0.491%, COV_{IMEP} 0.781%, and $COV_{q_{max}}$ 2.640%, respectively, which were lower than those obtained at point 1100/25. At the 1800/70 point, HVO showed an increase in $COV_{p_{max}}$ relative to DF by 128.78% (1.122%), whereas HVO + WPPO showed an increase of 56.23% (0.767%). For COV_{IMEP}, the differences were, respectively, 156.88% increase for HVO (2.006%) and 44.06% increase for HVO + WPPO (1.125%). The smallest differences relative to DF were observed for $COV_{q_{max}}$. For HVO, there was an increase of 46.12% (3.858%), whereas for HVO + WPPO it increased by 17.81% (3.110%). It is noteworthy that all analyzed parameters showed a coefficient of variation of less than 4% for $COV_{q_{max}}$, to about 2% for COV_IMEP, and less than 1.15% for the most analyzed parameter $COV_{p_{max}}$. Although the tests at the two points in the WHSC cycle showed differences in the average values and their coefficients of variation, they were not sufficiently large to exclude the proposed fuel from use in the engine. Owing to the lack of literature in the area covering this study, the results of other researchers were not referenced.

Because of the small number of analyzed values (100 points) for each test point, 10 classes were used in the distribution analysis. A non-parametric kernel-smoothing distribution was used for the analysis. Histograms were plotted to fit the density function, which could indicate multimodality in addition to asymmetry (Fig. 6 and Fig. 7). Although for the most part the distributions were close to normal, a few slightly bi-modal distributions also became apparent (e.g., p_{max} at HVO and HVO + WPPO feeds and IMEP for HVO + WPPO).

In the statistical analysis, kurtosis values κ were determined using MATLAB software (Table 5), and the distributions of the analyzed values were compared to a normal distribution. The lowest κ value 1.87 was found for q_{max} when the HVO was fed at test point 1800/70. This indicates the presence of a platykurtic. The vast majority of kurtosis values for both test points of operation were close to 3, which is the reference value of a normal distribution.

The second parameter used to assess the shape of the distribution of the analyzed values was the skewness s. In this case, the reference value was zero, indicating the normality of the distribution. In the analyzed cases (Table 5), the values were variably located in both the left and right areas, with small deformations. The maximum value of the skewness of the distribution (–0.32) was found for the IMEP at the HVO + WPPO feed at test point 1100/25. In addition, in the case of p_{max} itself, s was shown at –0.23, which confirms the asymmetry of the distribution.

One-way ANOVA [28] was used for the final statistical evaluation. The resulting groups were divided with respect to the fuels and study points, and MATLAB was used for the calculations. The null hypothesis was accepted, according to which the mean values in each group at each test point were derived from a population with the same mean value (Eq. (9))

$$H_0: \quad \bar{x}_{DF} = \bar{x}_{HVO} = \bar{x}_{HVO+WPPO} \tag{9}$$

According to the null hypothesis, the alternative hypothesis assumes that the averages of the analyzed populations are not equal (Eq. (10)).

$$H_1: \quad \bar{x}_{DF} \neq \bar{x}_{HVO} \neq \bar{x}_{HVO+WPPO} \tag{10}$$

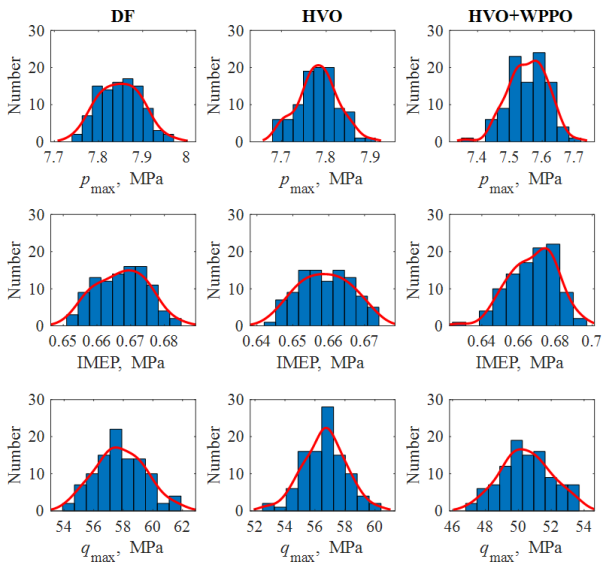

Fig. 6. Distributions of analyzed parameters at operating point 1100/25

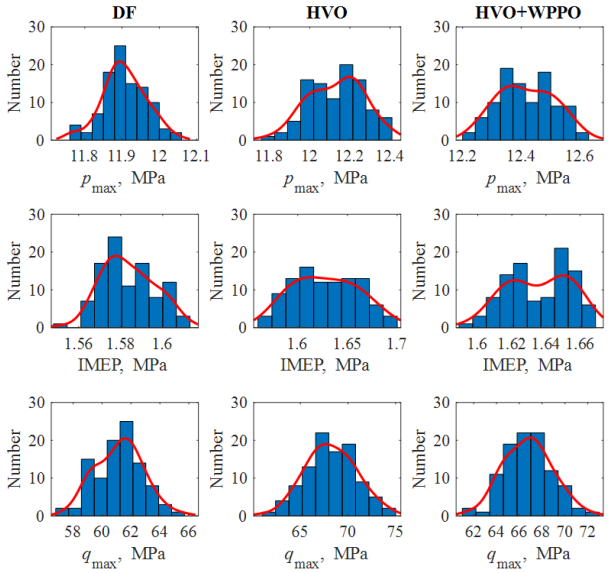

Fig. 7. Distributions of analyzed parameters at test operating 1800/70

Table 5. Comparative values of the kurtosis (κ) and skewness (s) at both operating points

operat. point		1100/25			1800/70		
fuel/ parameter		DF	HVO	HVO + WPPO	DF	HVO	HVO + WPPO
κ	p_{max}	2.5201	2.2559	2.6085	3.0940	2.4435	2.7119
	IMEP	2.8825	2.1528	3.1978	2.4370	2.1043	2.7506
	q_{max}	3.1465	2.9538	2.5597	2.0869	1.8698	2.8415
s	p_{max}	0.1041	0.0311	–0.2306	–0.0463	–0.1781	0.0677
	IMEP	–0.0080	–0.0039	–0.3209	0.2053	0.1232	–0.1693
	q_{max}	0.1117	–0.1392	0.0373	0.0686	0.0392	0.0932

Box plots (Fig. 8 and Fig. 9) highlighted differences in the location of mean values, clustering (25th and 75th percentile), and whiskers resulting from the spread of the analyzed values. A summary of the ANOVA is presented in Table 6, which includes the variance. SS represents the sum of squares, and df represents the degrees of freedom. The values of the mean square error MS clearly indicate low values relative to the mean values of the analyzed parameters. The statistic F was the quotient of the mean squares. The final probability values prob > F for all analyzed values and test points clearly indicate that the sample statistics did not reach the accepted threshold F. The highest value was reached for the IMEP at test point 1100/20 and was 1.01×10^{-11}, which is very low in relation to the limit derived from the 95% confidence threshold, which is 0.05. The remaining values prob > F were well below those indicated for the IMEP. This means that, in all the cases analyzed, the hypothesis H_0 (Eq. (9)) showing agreement of mean values, should be rejected in favor of the alternative hypothesis H_1 (Eq. (10)) indicating that the population means were different.

Because the distributions shown in (Fig. 6 and Fig. 7) showed possible discrepancies from the normal distribution, an additional statistical test was performed. In such cases, it was expedient to use Levene, Brown-Forsythe and O'Brien absolute tests [9]. As with the ANOVA, MATLAB software was used. The essence of the test is to show that the probability p of the test (f_{stat}) is in the range (0...1), with a value of 1 indicating acceptance of the hypothesis H_0 (Eq. (9)). All the p values determined in the course of the analysis, shown in Table 7, show small values, which indicates the fact that the alternative hypothesis H_1 has been accepted as valid, indicating the significance of the differences in the mean values of the analyzed parameters at the test points.

Based on the results of the calculations and analyses presented in this paper, it was concluded that this goal was achieved. The proposed HVO + WPPO alternative fuel has slightly different ignition and combustion characteristics and engine stability compared with DF. Tests at two points in the WHSC cycle showed differences in the average values of p_{max}, IMEP, q_{max}, and their COV coefficients of variation, but they were not large enough to exclude the proposed fuel from use in the engine. The dependence of the differences in the analyzed parameters on the load and engine speed was also determined. These findings highlight the need for further research in this area.

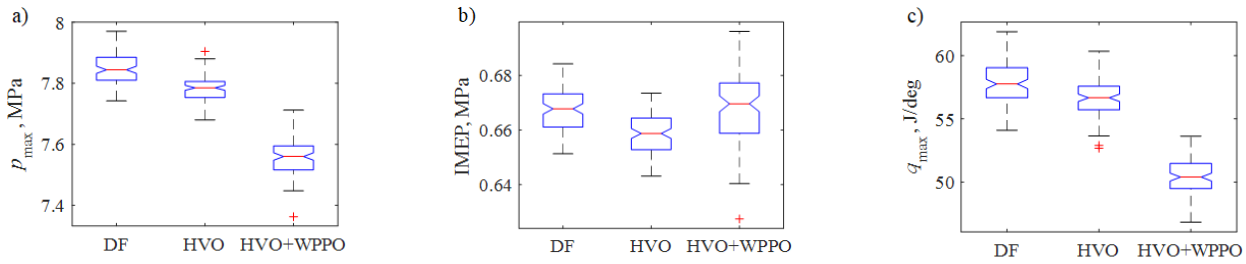

Fig. 8. Box plots indicating the location of the analyzed values at operating point 1100/25

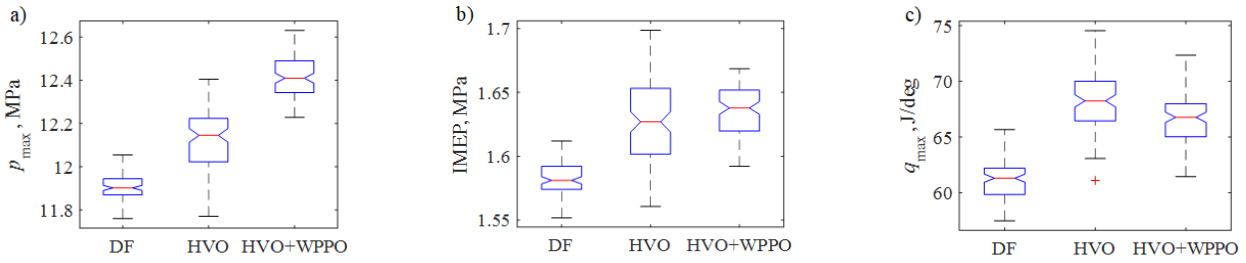

Fig. 9. Box plots indicating the location of the analyzed values at operating point 1800/70

Table 6. Summary ANOVA statistics of the values analyzed at both operating points

RPM/load		1100/25					1800/70				
Parameter	Source	SS	df	MS	F	Prob > F	SS	df	MS	F	Prob > F
p_{max}	Columns	4.68900	2	2.3445	907.46	3.09×10^{-127}	13.04260	2	6.5213	631.00	1.17×10^{-107}
	Error	0.76732	297	0.00258			3.06950	297	0.01034		
	Total	5.45630	299				16.11210	299			
IMEP	Columns	0.00497	2	0.00248	27.60	1.01×10^{-11}	0.15672	2	0.07836	150.89	6.03×10^{-46}
	Error	0.02672	297	9.00×10^{-5}			0.15424	297	5.20×10^{-4}		
	Total	0.03169	299				0.31097	299			
q_{max}	Columns	3097.50	2	1548.75	647.79	4.92×10^{-109}	2745.75	2	1372.88	297.58	1.16×10^{-71}
	Error	710.07	297	2.3908			1370.20	297	4.6135		
	Total	3807.57	299				4115.96	299			

Table 7. Summary Levene'a, Browna-Forsythe'a and O'Briena tests of the values analyzed at both operating points

Parameter		1100/25	1800/70
p_{max}	p	0.0049	1.1059×10^{-15}
	f_{stat}	5.4099	38.7588
IMEP	p	6.6987×10^{-10}	1.0665×10^{-21}
	f_{stat}	22.7002	57.0665
q_{max}	p	0.1436	4.5403×10^{-5}
	f_{stat}	1.9535	10.3443

4. Conclusions

In this study, three types of diesel fuel were compared: conventional diesel fuel (DF), hydrotreated vegetable oil (HVO), and a mixture of HVO with PPO and PSO additives (HVO + WPPO). Measurements were carried out on a special platform with a research engine at two points of the World Harmonized Stationary Cycle (WHSC) 1100/25 and 1800/70. Based on the measurements, calculations, and analysis, the following conclusions were drawn.

1. HVO and HVO + WPPO have slightly different combustion patterns than the conventional DF. In the case of HVO, this may be due to the higher reactivity of the fuel, which affects engine performance. HVO + WPPO has shown similar performance to DF, which is the rationale for its use in engines.
2. The average maximum pressure values at the 1100/25 point were 7.848, 7.781, and 7.556 MPa for DF, HVO, and HVO + WPPO, respectively. In contrast, at test point 1800/70, DF 11.906 MPa HVO 12.13MPa, HVO + WPPO 12.42 MPa. The values obtained were not significantly different.
3. The average values of the indicated mean effective pressure at the 1100/25 point were 0.667, 0.659, and 0.668 MPa for DF, HVO, and HVO + WPPO, respectively. However, at test points 1800/70, DF was 1.584 MPa, HVO was 1.628 MPa, and HVO + WPPO was 1.636 MPa. The values obtained were not significantly different.
4. The averaged maximum heat release values at the 1100/25 point were for DF 57.80 J/deg, HVO 56.61 J/deg MPa, and with HVO + WPPO 50.47 J/deg. In contrast, at test point 1800/70, DF 61.18 J/deg HVO 68.203 J/deg, HVO + WPPO 66.74 J/deg. The values obtained also do not provide a basis for rejecting HVO + WPPO from use in the engine.
5. The coefficients of variation of the analyzed parameters indicate the stability of the engine's operation, only in the case of heat generation approaching 4%, in other cases, they rarely reached 2%. Based on the small values of the coefficients of variation, the percentage differences often exceeded 50%.
6. 6 Statistical analyses, including ANOVA and Levene's tests, confirmed significant differences between the fuels, indicating the potential of the HVO + WPPO mixture as an environmentally friendly alternative to DF, especially at higher speeds and loads.

Acknowledgements

The research leading to these results has received funding from the commissioned task entitled “Polytechnic Network VIA CARPATIA named after President of the Republic of Poland Lech Kaczynski”, financed by a special purpose grant from the Minister of Science and Higher Education contract no: MEiN/2022/DPI/2575, MEiN/2022/DPI/2577, MEiN/2022/DPI/2578, activity “ISKRA – building inter-university research teams”.

Nomenclature

BMEP brake mean effective pressure
CAD crank angle degree
CO carbon monoxide
CO_2 carbon dioxide

COV	cycle-by-cycle variations
DF	diesel fuel
FTIR	Fourier-transform infrared
HC	hydrocarbon
HVO	hydrotreated vegetable oil
IMEP	indicated mean effective pressure
NO_x	nitrogen oxides
PM	particulate matter
PPO	polypropylene oil
PSO	polystyrene oil
THC	total hydrocarbon
TPO	automobile tire oil
WHSC	World Harmonized Stationary Cycle
WPPO	waste plastic pyrolysis oils
$\bar{x}$	mean value of the parameter under study
κ	kurtosis
p	maximum pressure in the cylinder
q	heat released in the cylinder
s	skewness
σ	standard deviation

Bibliography

[1] Ananthakumar S, Jayabal S, Thirumal P. Investigation on performance, emission and combustion characteristics of variable compression engine fuelled with diesel, waste plastics oil blends. J Brazilian Soc Mech Sci Eng. 2017;39(1): 19-28. https://doi.org/10.1007/s40430-016-0518-6

[2] Azeem N, Beatrice C, Vassallo A, Pesce F, Gessaroli D, Biet C et al. Experimental study of cycle-by-cycle variations in a spark ignition internal combustion engine fueled with hydrogen. Int J Hydrogen Energy. 2024;60:1224-1238. https://doi.org/10.1016/j.ijhydene.2024.02.182

[3] Bortel I, Vávra J, Takáts M. Effect of HVO fuel mixtures on emissions and performance of a passenger car size diesel engine. Renew Energy. 2019;140:680-691. https://doi.org/10.1016/j.renene.2019.03.067

[4] Budsaereechai S, Hunt AJ, Ngernyen Y. Catalytic pyrolysis of plastic waste for the production of liquid fuels for engines. RSC Adv. 2019;9(10):5844-5857. https://doi.org/10.1039/C8RA10058F

[5] Channappagoudra M, Ramesh K, Manavendra G. Comparative study of standard engine and modified engine with different piston bowl geometries operated with B20 fuel blend. Renew Energy. 2019;133:216-232. https://doi.org/10.1016/j.renene.2018.10.027

[6] Das AK, Hansdah D, Mohapatra AK, Panda AK. Energy, exergy and emission analysis on a DI single cylinder diesel engine using pyrolytic waste plastic oil diesel blend. J Energy Inst. 2020;93(4):1624-1633. https://doi.org/10.1016/j.joei.2020.01.024

[7] Devi DS, Kumar R, Rajak U. Experimental investigation of performance, emission and combustion characteristics of a CI engine fuelled by blends of waste plastic oil with diesel. Energy Sources, Part A Recover Util Environ Eff. 2022;44: 7693-7708. https://doi.org/10.1080/15567036.2022.2115582

[8] Faisal F, Rasul MG, Jahirul MI, Chowdhury AA. Waste plastics pyrolytic oil is a source of diesel fuel: A recent review on diesel engine performance, emissions, and combustion characteristics. Sci Total Environ. 2023;886:163756. https://doi.org/10.1016/j.scitotenv.2023.163756

[9] Gastwirth JL, Gel YR, Miao W. The impact of Levene's Test of equality of variances on statistical theory and practice. Stat Sci. 2009;24(3):343-360. https://doi.org/10.1214/09-STS301

[10] Heng Teoh Y, Geok How H, Wen Lee S, Lin Loo D, Danh Le T, Tho Nguyen H et al. Optimization of engine out responses with different biodiesel fuel blends for energy transition. Fuel. 2022;318:123706. https://doi.org/10.1016/j.fuel.2022.123706

[11] Huang Z, Huang J, Luo J, Hu D, Yin Z. Performance enhancement and emission reduction of a diesel engine fueled with different biodiesel-diesel blending fuel based on the multi-parameter optimization theory. Fuel. 2022;314: 122753. https://doi.org/10.1016/j.fuel.2021.122753

[12] Hunicz J, Krzaczek P, Gęca M, Rybak A, Mikulski M. Comparative study of combustion and emissions of diesel engine fuelled with FAME and HVO. Combustion Engines. 2021;184(1):72-78. https://doi.org/10.19206/ce-135066

[13] Jakubowski M, Jaworski A, Kuszewski H, Balawender K. Performance of a diesel engine fueled by blends of diesel fuel and synthetic fuel derived from waste car tires. Sustain. 2024;16(15):6404. https://doi.org/10.3390/su16156404

[14] Januszewicz K, Hunicz J, Kazimierski P, Rybak A, Suchocki T, Duda K et al. An experimental assessment on a diesel engine powered by blends of waste-plastic-derived pyrolysis oil with diesel. Energy. 2023;281:128330. https://doi.org/10.1016/j.energy.2023.128330

[15] Krzemiński A, Ustrzycki A. Visualisation testing of the vertex angle of the spray formed by injected diesel–ethanol fuel blends. Energies. 2024;17(12):3012. https://doi.org/10.3390/en17123012

[16] Li X, Liu Q, Ma Y, Wu G, Yang Z, Fu Q. Simulation study on the combustion and emissions of a diesel engine with different oxygenated blended fuels. Sustain. 2024;16(2):631. https://doi.org/10.3390/su16020631

[17] McCaffery C, Zhu H, Sabbir Ahmed CM, Canchola A, Chen JY, Li C et al. Effects of hydrogenated vegetable oil (HVO) and HVO/biodiesel blends on the physicochemical and toxicological properties of emissions from an off-road heavy-duty diesel engine. Fuel. 2022;323:124283. https://doi.org/10.1016/j.fuel.2022.124283

[18] Mussa NS, Toshtay K, Capron M. Catalytic applications in the production of hydrotreated vegetable oil (HVO) as a renewable fuel: a review. Catalysts. 2024;14(7):452. https://doi.org/10.3390/catal14070452

[19] Pietras D, Stelmasiak Z, Pietras P. Comparison of operational parameters and stability of performance of an automotive SI engine powered by methyl and ethyl alcohols. Combustion Engines. 2023;194(3):129-140. https://doi.org/10.19206/CE-169136

[20] Preuß J, Munch K, Denbratt I. Performance and emissions of renewable blends with OME3-5 and HVO in heavy duty and light duty compression ignition engines. Fuel. 2021;303: 121275. https://doi.org/10.1016/j.fuel.2021.121275

[21] Prokopowicz A, Zaciera M, Sobczak A, Bielaczyc P, Woodburn J. The effects of neat biodiesel and biodiesel and HVO blends in diesel fuel on exhaust emissions from a light duty vehicle with a diesel engine. Environ Sci Technol. 2015;49(12):7473-7482. https://doi.org/10.1021/acs.est.5b00648

[22] Rybak A, Hunicz J, Szpica D, Mikulski M, Gęca M, Woś P. Comparative analysis of waste-derived pyrolytic fuels applied in a contemporary compression ignition engine. Combustion Engines. 2024;198(3):74-81. https://doi.org/10.19206/CE-186697

[23] Sharma P, Dhar A. Effect of hydrogen fumigation on combustion stability and unregulated emissions in a diesel fuelled compression ignition engine. Appl Energy. 2019; 253:113620. https://doi.org/10.1016/j.apenergy.2019.113620

[24] Singh RK, Ruj B, Sadhukhan AK, Gupta P, Tigga VP. Waste plastic to pyrolytic oil and its utilization in CI engine: performance analysis and combustion characteristics. Fuel. 2020;262:116539. https://doi.org/10.1016/j.fuel.2019.116539

[25] Sitnik LJ, Sroka ZJ, Andrych-Zalewska M. The impact on emissions when an engine is run on fuel with a high heavy alcohol content. Energies. 2021;14(1):41. https://doi.org/10.3390/en14010041

[26] Suarez-Bertoa R, Kousoulidou M, Clairotte M, Giechaskiel B, Nuottimäki J, Sarjovaara T et al. Impact of HVO blends on modern diesel passenger cars emissions during real world operation. Fuel. 2019;235:1427-1435. https://doi.org/10.1016/j.fuel.2018.08.031

[27] Tutak W, Jamrozik A, Pyrc M. Experimental investigations on combustion, performance and emissions characteristics of compression ignition engine powered by B100/ethanol blend. E3S Web of Conferences. EDP Sciences 2017;14: 02019. https://doi.org/10.1051/e3sconf/20171402019

[28] Vural E, Özer S, Özel S, Binici M. Analyzing the effects of hexane and water blended diesel fuels on emissions and performance in a ceramic-coated diesel engine by Taguchi optimization method. Fuel. 2023;344:128105. https://doi.org/10.1016/j.fuel.2023.128105

[29] Zhang Z, Li J, Tian J, Dong R, Zou Z, Gao S et al. Performance, combustion and emission characteristics investigations on a diesel engine fueled with diesel/ethanol/n-butanol blends. Energy. 2022;249:123733. https://doi.org/10.1016/j.energy.2022.123733

[30] Zhang Z, Ye J, Tan D, Feng Z, Luo J, Tan Y et al. The effects of Fe_2O_3 based DOC and SCR catalyst on the combustion and emission characteristics of a diesel engine fueled with biodiesel. Fuel. 2021;290:120039. https://doi.org/10.1016/j.fuel.2020.120039

Dariusz Szpica, DSc., DEng. – Faculty of Mechanical Engineering, Bialystok University of Technology, Poland.
e-mail: *d.szpica@.pb.edu.pl*

Mirosław Jakubowski, DEng. – Faculty of Mechanical Engineering and Aeronautics, Rzeszow University of Technology, Poland.
e-mail: *mjakubow@prz.edu.pl*

Michał S. Gęca, DSc., DEng. – Faculty of Mechanical Engineering, Lublin University of Technology, Poland.
e-mail: *michal.geca@pollub.pl*

Artur Krzemiński, DEng. – Faculty of Mechanical Engineering and Aeronautics, Rzeszow University of Technology, Poland.
e-mail: *akrzeminski@prz.edu.pl*

Prof. Jacek Hunicz, DSc., DEng. – Faculty of Mechanical Engineering, Lublin University of Technology, Poland.
e-mail: *j.hunicz@pollub.pl*

Grzegorz Mieczkowski, DSc., DEng. – Faculty of Mechanical Engineering, Bialystok University of Technology, Poland.
e-mail: *g.mieczkowski@pb.edu.pl*